

Efficient “Light-soaking”-free Inverted Organic Solar Cells with Aqueous Solution Processed Low-Temperature ZnO Electron Extraction Layers

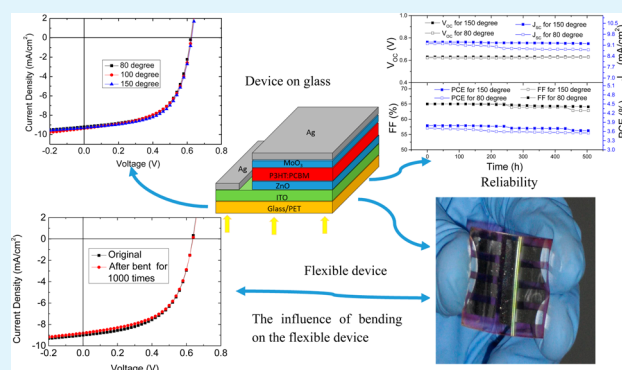
Wei Wei,[†] Chunfu Zhang,^{*,†} Dazheng Chen,[†] Zhizhe Wang,[†] Chunxiang Zhu,[‡] Jincheng Zhang,[†] Xiaoli Lu,[†] and Yue Hao^{*,†}

[†]State Key Laboratory of Wide Bandgap Semiconductor Technology School Of Microelectronics, Xidian University, 2 South Taibai Road, Xi'an, China 710071

[‡]Department of Electrical and Computer Engineering, National University of Singapore, 10 Kent Ridge Crescent, Singapore 119260, Singapore

ABSTRACT: Low-temperature processes are unremittingly pursued in the fabrication of organic solar cells. The paper reports that the highly efficient and “light-soaking”-free inverted organic solar cell can be achieved by using ZnO thin films processed from the aqueous solution method at a low temperature. The inverted organic solar with an aqueous-processed ZnO thin film annealed at 150 °C shows an efficiency of 3.79%. Even when annealed at a temperature as low as 80 °C, the device still shows an efficiency of 3.71%. With the proper annealing temperature of 80 °C, the flexible device, which shows an efficiency of 3.56%, is fabricated on PET. This flexible device still keeps the efficiency above 3.40% after bent for 1000 times with a curvature radius of 50 mm. In contrast, a low annealing temperature leads to an inferior device performance when the ZnO thin film is processed from the widely used sol–gel method. The device with sol–gel processed ZnO annealed at 150 °C only shows a PCE of 1.3%. Furthermore, the device shows a strong “light-soaking” effect, which is not observed in the device containing an aqueous-processed ZnO thin film. Our results suggest that the adopted aqueous solution method is a more efficient low temperature technique, compared with the sol–gel method.

KEYWORDS: aqueous solution method, inverted organic solar cell, zinc oxide, sol gel method, “light-soaking” effect



INTRODUCTION

Polymer organic solar cells attract more and more attentions recently and their performances have been improved dramatically in the past 10 years. The highest power conversion efficiency (PCE) of a single junction organic solar cell can be over 8%,¹ and a tandem polymer solar cell can reach the PCE higher than 10%² nowadays.

Conventional organic solar cells contain a photoactive organic blend layer sandwiched between an anode buffer layer, typically poly(3,4-ethylenedioxythiophene)–poly(styrenesulfonate) (PEDOT:PSS), and a low work-function metal, typically Al. However, because PEDOT:PSS is acidic, which will influence the stability of the active layer, and the top low work function metal layer is sensitive to oxygen, the performance of the conventional device degrades very quickly.^{3–6}

Inverted organic solar cells are more appealing for their comparable PCEs and improved stabilities.^{7–9} In this structure, *n*-type materials, such as ZnO, TiO₂, and Cs₂CO₃, are usually used as a cathode buffer layer to make ITO more effective as an electron collecting electrode. Among these materials, ZnO is

more attractive for its high electron mobility, environmentally friendly nature, Ohmic contact with the organic layer, and good optical transmittance. To deposit a thin layer of ZnO in inverted organic solar cells, different methods, including the magnetron sputter, MOCVD, CVD, ALD, sol–gel, and ZnO nanoparticle methods,^{1,8,10,11} can be used. Among them, the solution processed method is more desirable, since it is time saving, low cost, simple, and compatible with printing techniques.

The sol–gel method is the most widely used solution method in the inverted solar cell.^{12,13} In this method, to achieve a high PCE, a high temperature, usually 200–400 °C, is needed to anneal the processed ZnO film. Lowering the annealing temperature will lead to a worse and worse device performance. However, a low process temperature is always preferred, which not only saves energy budget but also make possible the fabrication of flexible solar cells (flexible substrates such as PET

Received: September 30, 2013

Accepted: December 5, 2013

Published: December 5, 2013

usually cannot withstand a temperature higher than 200 °C). Though the ZnO thin film can be efficiently made at a very low temperature by the ZnO nanoparticle method, its precursor solution is not stable enough.¹⁴

In this work, an aqueous solution method is adopted to synthesize the ZnO film at a very low temperature. In 2008, this method was adopted by Keszler et al.¹⁵ to synthesize ZnO at an annealing temperature of about 150 °C in TFT. Later on, some other literatures^{11,16} used the similar method to synthesize the ZnO film in the inverted organic solar cell. On the basis of these works, the annealing temperature is lowered further and, ultimately, the flexible organic solar cell is fabricated on polyethylene terephthalate (PET). Compared to the device with the sol-gel processed ZnO film, the device with the aqueous solution processed low temperature ZnO film shows an obvious superior performance, even with a lower temperature. For the sol-gel method, the device on glass with a 150 °C annealed ZnO film shows a PCE of only 1.3%. For the aqueous solution method, the device on glass with a 150 °C annealed ZnO shows a PCE of 3.79%, and when the ZnO layer is annealed at 100 °C, the device shows a PCE of 3.75%. Even when the ZnO layer is annealed at 80 °C, the device still shows a very high PCE of 3.71%. The aqueous solution method is further used to synthesize the ZnO layer at 80 °C in the flexible organic solar cell, which shows a comparably high PCE of 3.56%, and the PCE still remains above 3.40% after the device is bent for 1000 times with a curvature radius of 50 mm. Furthermore, with a sol-gel processed ZnO layer, the device shows a strong “light-soaking” effect, while no obvious “light-soaking” effect is observed in devices with an aqueous solution processed ZnO film.

EXPERIMENTAL DETAIL

Devices containing the sol-gel and aqueous solution processed ZnO films are fabricated.

For the sol gel method, zinc acetate dehydrate [$\text{Zn}(\text{CH}_3\text{COO})\cdot 2\text{H}_2\text{O}$] (99.9%, Sigma-Aldrich) was prepared as the precursor and mixed ethanol [$\text{CH}_3\text{CH}_2\text{OH}$] (99.5% Aldrich) as the solvent. The concentration of zinc acetate dehydrate is 0.1 M. Subsequently, ethanolamine [$\text{NH}_2\text{CH}_2\text{CH}_2\text{OH}$] (99% Sigma-Aldrich) was added to the solution as a sol stabilizer. Then, the solution was heated to 80 °C and magnetically stirred for more than 20 h for thorough mixing as our previous report.¹⁷

For the aqueous solution method, ZnO powder (99.9%, particle size <5 μm , Sigma-Aldrich) was dissolved in ammonia (25%, Tianjin Chemical Reagent Co.) to form 0.1 M ($\text{Zn}(\text{NH}_3)_4^{2+}$) solutions. The solution was ultrasonically processed for 3–5 min and then stored at 0–10 °C for more than 12 h before use.

Figure 1 shows the layer structure of the device and the corresponding energy diagram of the device. The fabrication processes were as follows: The patterned ITO-coated glass (the thickness of ITO is 120 nm and the sheet resistance $\leq 10 \Omega/\square^{-1}$) was first ultrasonicated in detergent, deionized water, acetone and ethyl alcohol each for 10 min and was subsequently blown dry with a nitrogen gun. The sol-gel or aqueous precursor solution was then spin-cast onto cleaned ITO-glass substrates at 3000 rpm for 40 s, followed by annealing in the oven under ambient conditions for 30 min. The solution of poly-3-hexylthiophene (P3HT) and [6,6]-phenyl-C61-butyric acid methyl ester (PCBM) in 1,2-chlorobenzene with the concentration of 20 mg/mL and 1:0.8 weight ratio was spin-cast on the top of ZnO films at 1000 rpm for 60 s to form the active layer. The devices were then preannealed at 150 °C for 10 min. Finally, the MoO_3/Ag anode was thermally evaporated onto the top of the active layer through a shadow mask in a vacuum of about 4×10^{-6} Torr. The thicknesses of MoO_3 and Ag were 80 Å and 1000 Å separately and the active area of the solar cell was about 12 mm^2 .

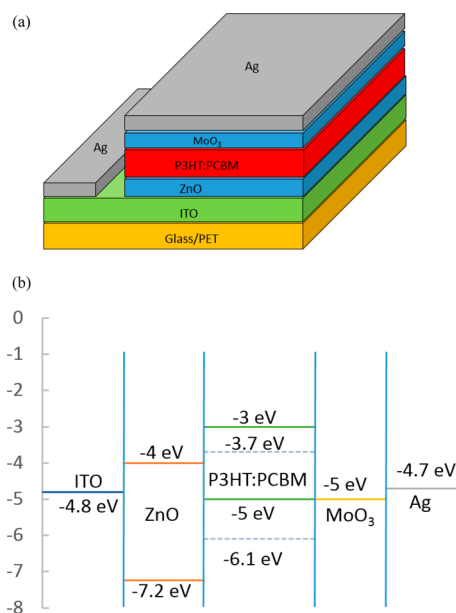


Figure 1. (a) Schematic illustration of the inverted organic solar cell with the configuration of Glass or PET/ITO/ZnO/P3HT:PCBM/ MoO_3/Ag . (b) Corresponding energy diagram of the materials for the device.

Our flexible substrate, (PET), has an ITO thin film (the thickness of PET-ITO is about 0.15 μm and the sheet resistance $\leq 60 \Omega/\square^{-1}$) on its top. For the device on PET, the fabrication processes are the same as above.

Tapping mode AFM tests were performed to test the ZnO layer by an Agilent 5500 scanning probe system. A Keithley 2400 source-measure unit and a Xenon lamp (XEC-300M2, SANEI ELECTRIC) with an AM 1.5G filter were utilized to measure the current density–voltage (J – V) characteristics of all the devices in air. The light intensity was adjusted to 100 mW/cm^2 illumination by a standard solar cell calibrated by the National Renewable Energy Laboratory (NREL). The thickness and the transmittance spectra of the ZnO layers were determined by a spectroscopic ellipsometry (ESM-300, J.A. Woollam Co. Inc.). The photoluminescence (PL) spectrum test was also performed to analyze the ZnO thin film using the 325-nm line of a He–Cd laser.

RESULTS AND DISCUSSION

To pursue the low temperature device fabrication processes, a low temperature of 150 °C was first utilized to anneal the layer of ZnO processed from the sol-gel method, and the device performance is shown in Figure 2. It can be seen that the “light-soaking” effect is strong in the device with the sol-gel processed ZnO layer. Researches have indicated that the origin of the “light-soaking” effect lies on the nature of the metal-oxide/organic interface.^{18,19} The UV light can rearrange the Fermi level of the metal-oxide and thus reduce the trapped charges at the interface, so the performance will restore after soaking in light.^{18,19} Our results show the same trend, as shown in Figure 2. The original PCE of the device is only 0.2%, while the PCE saturates at about 1.3% after being soaked in light for about 10 min. As indicated in Table 1, the short circuit current density (J_{SC}) and fill factor (FF) all increase dramatically with the light soaking time, and the open circuit voltage (V_{OC}) is also improved slightly. All these phenomena are typical in the “light-soaking” effect.^{18,19} The saturated PCE of 1.3% is relatively lower than that of the device with 350 °C annealed ZnO, where a PCE of 2.82% was achieved in our previous

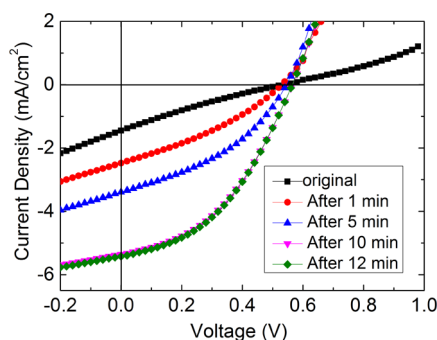


Figure 2. J – V characteristics of the inverted organic solar cell after a different light soaking time ranging from 0 to 10 min. The ZnO film was derived from a sol–gel concentration of 0.1 M followed by annealed at 150 °C. The tests were under an AM 1.5G illumination of 100 mW/cm².

Table 1. Variation of Parameters of the Device with the Light Soaking Time^a

light soaking time (min)	V_{OC} (V)	J_{SC} (mA/cm ²)	FF (%)	PCE (%)
0 (Original)	0.52	−1.76	21	0.20
1	0.52	−2.87	34	0.51
5	0.54	−3.81	39	0.81
10	0.56	−5.36	43	1.29
12	0.56	−5.35	43	1.29

^aThe ZnO layer was derived from the sol–gel method, followed by annealed at 150 °C.

work.¹⁷ A low ZnO annealing temperature in sol–gel method not only greatly decreased the device PCE but also leads to the severe “light-soaking” effect.

Compared with the device containing a layer of sol–gel processed ZnO, the device with the aqueous solution processed ZnO layer shows an obviously improved performance as shown in Figure 3. PCE as high as 3.79% is achieved when the

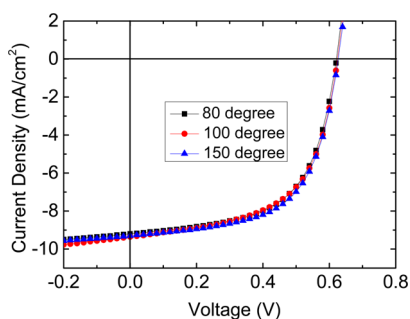


Figure 3. J – V characteristics of the inverted organic solar cells containing aqueous solution derived ZnO layers annealed at 150 °C, 100 °C, and 80 °C, under an AM 1.5G illumination of 100 mW/cm². The device containing a 150 °C annealed ZnO layer shows a PCE of 3.79%, the device with a 100 °C annealed ZnO layer shows a PCE of 3.75%, the device with an 80 °C annealed ZnO layer shows a PCE of 3.71%.

aqueous-processed ZnO layer is annealed at 150 °C. For this device, V_{OC} of 0.63 V, J_{SC} of 9.3 mA/cm², FF of 65%, the series resistance (R_S) of 0.6 Ω ·cm², and the shunt resistance (R_{SH}) of 691 Ω ·cm² are obtained. Furthermore, no obvious light-soaking effect is observed in this device. For the aqueous-processed ZnO annealed at 100 °C, the device still shows a very high performance with V_{OC} of 0.63 V, J_{SC} of 9.3 mA/cm², FF of 64%,

and an overall PCE of 3.75%. Even for the aqueous-processed ZnO annealed at 80 °C, the device containing it still shows a very high performance with V_{OC} of 0.62 V, J_{SC} of 9.2 mA/cm², FF of 65%, and an overall PCE of 3.71%, which is only slightly lower than that of the device with a ZnO film annealed at 100 or 150 °C. R_S only slightly increases from 0.6 Ω ·cm² (150 °C) to 0.8 Ω ·cm² (100 °C) and finally to 0.9 Ω ·cm² (80 °C), which is one reason for a slightly lower FF at a lower annealing temperature. No obvious “light-soaking” effect is observed in devices with aqueous processed ZnO films annealed at different temperatures. Since the flexible substrate cannot withstand a high annealing temperature, a low annealing temperature of 80 °C is definitely a better choice for future flexible device fabrication. Anyway, for the device with the ZnO film annealed at low temperature, the aqueous solution method shows an obvious superior behavior.

After the performance of devices on glass is researched, the cells are fabricated on PET, which is a flexible substrate. The aqueous solution processed ZnO is annealed at a low temperature of 80 °C. The photo of the flexible devices is shown in Figure 4a, and the size of the PET substrate is 35 mm

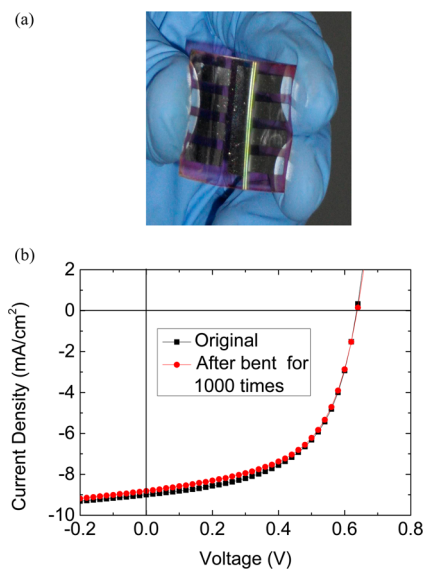


Figure 4. (a) Photo of our flexible solar cell. (b) J – V characteristics of the device before and after the device is bent for 1000 times. The bending radius is about 50 mm. The original device shows a V_{OC} of 0.64 V, J_{SC} of 9.0 mA/cm², FF of 62%, and PCE of 3.56%. After being bent, the device shows a V_{OC} of 0.64 V, J_{SC} of 8.8 mA/cm², FF of 61%, and PCE of 3.43%.

× 25 mm. In order to examine the influence of bending on the device, the PET substrate is bent with a curvature radius of 50 mm. Figure 4b shows J – V characteristics of the original device and the device after the substrate is bent for 1000 times. Compared with the similar device on glass with a PCE of 3.71%, the PCE of the original device on PET is 3.56%. The device shows a V_{OC} of 0.64 V, FF of 62%, and J_{SC} of 9.0 mA/cm². After being bent for 1000 times, the device shows a V_{OC} of 0.64 V, J_{SC} of 8.8 mA/cm², FF of 61%, and PCE of 3.43%. Therefore, the device shows superior flexibility, and the aqueous solution method is definitely a promising method for synthesizing functional ZnO thin layer in the device on the flexible substrate.

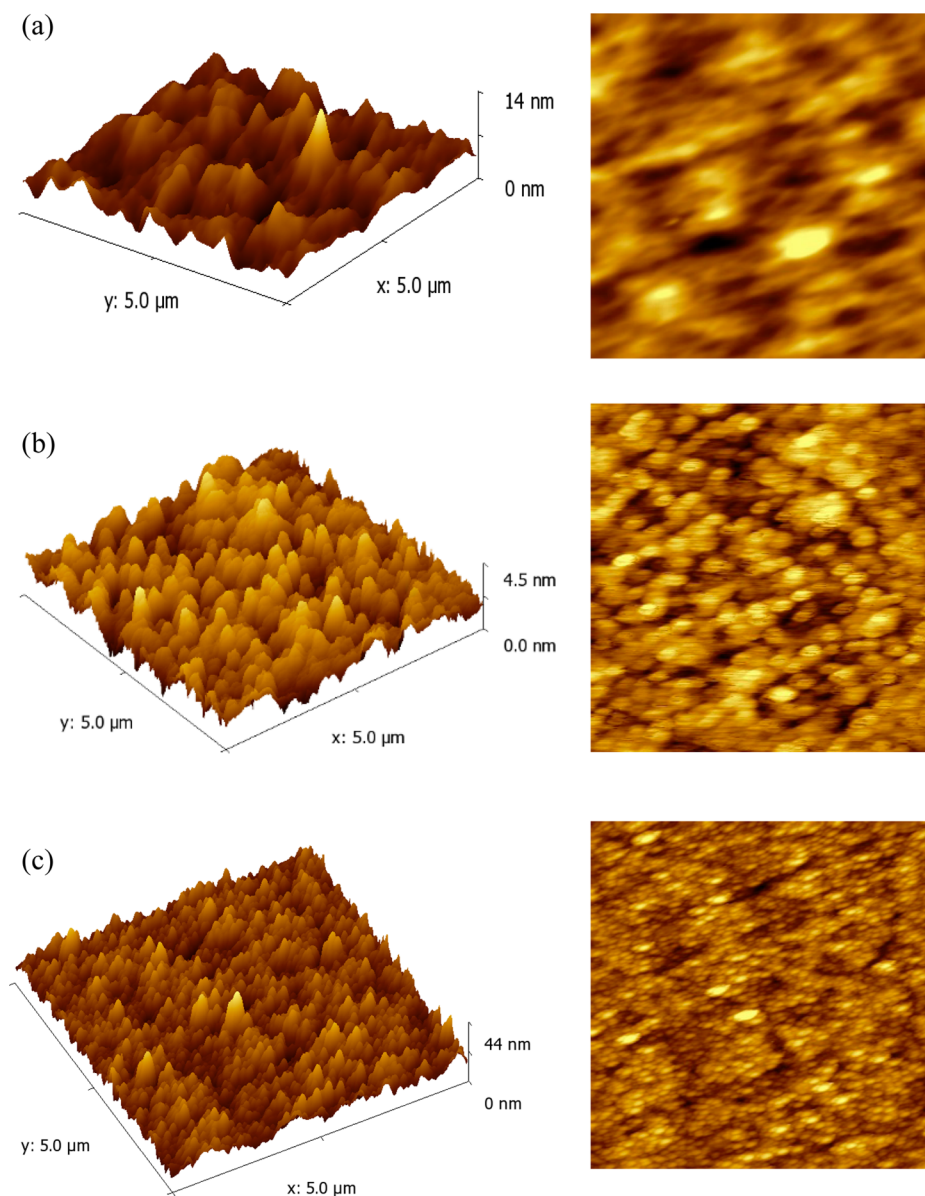


Figure 5. 3D view (left) and Planar view (right) AFM images of the ZnO layers derived from (a) the 150 °C sol-gel method, (b) the 150 °C aqueous solution method, (c) the 350 °C sol-gel method. RMS values are (a) 13.6 Å, (b) 6.12 Å, and (c) 45.5 Å.

To find the difference between the two solution methods, AFM tests were first made to analyze the surface morphology of ZnO. Figure 5 shows the tapping mode AFM images of the ZnO layer that was made by sol-gel and aqueous solution methods at a different annealing temperature. All the samples are on the glasses. The values of root-mean-square (RMS) surface roughness are 6.12 Å for the aqueous solution processed ZnO film annealed at 150 °C and 13.6 Å and 45.5 Å for the sol-gel method processed ZnO films annealed at 150 and 350 °C, respectively. The aqueous solution processed ZnO layer annealed at 150 °C owned the lowest roughness. Commonly, a lower surface roughness will lead to a larger D/A interfacial area and a lower defect density, and thus an improved FF, J_{SC} , V_{OC} , and finally PCE.²⁰ Therefore, the lower surface roughness of the aqueous solution processed ZnO layer is expected to lead to a higher efficiency of the device, which is consistent with the electrical characteristics of the devices.

Figure 6a shows the transmittance spectra of an ITO/Glass, a sol-gel processed ZnO-coated ITO/Glass and an aqueous

solution processed ZnO-coated ITO/Glass. For the ITO/Glass, a transmittance of 90% is achieved, while for ZnO-coated ITO/Glasses, the layer of ZnO slightly decreases the transmittance to about 88% for both samples. As shown in the insert in Figure 6a, there is an obvious shift of the transmittance edges for these three samples. The transmittance edge of ITO/Glass is located at the lowest wavelength and that of the aqueous solution processed ZnO-coated ITO/Glass is located at the longest wavelength. It is well-known that the transmittance edge (or to say the absorption edge) of a material is greatly related to its optical absorption properties. The material absorption coefficient α can be determined as $T \approx \exp(-\alpha d)$, where T is the transmittance of a film and d is the thickness of the film. The optical band gap is determined by $(\alpha h\nu)^2 = D^2(h\nu - E_g)$, where $h\nu$ is the photon energy, E_g is the optical band gap, and D is a constant. Thicknesses of ZnO layers made by the two methods are both about 15 nm. Figure 6b shows the plot of $(\alpha h\nu)^2$ versus $h\nu$. From this plot, E_g can be determined.¹¹ The band gaps of the materials are determined to be 3.30 eV (150 °C

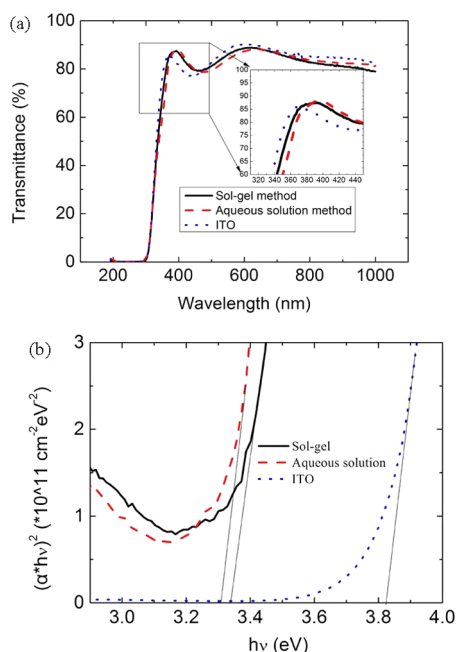


Figure 6. (a) Optical transmittance spectra of the ITO/Glass (blue dot line), the 150 °C aqueous solution processed ZnO-coated ITO/Glass (red dash line), and the 150 °C sol-gel processed ZnO-coated ITO/Glass (dark solid line). The highest transmittance is about 90% for the ITO/Glass, while the ZnO-coated ITO/Glasses show the highest transmittance of 88%. (b) The absorption coefficient as a function of photon energy. E_g (ZnO, 150 °C aqueous solution method) = 3.30 eV, E_g (ZnO, 150 °C sol-gel method) = 3.33 eV, and E_g (ITO) = 3.82 eV.

aqueous solution processed ZnO), 3.33 eV (150 °C sol-gel processed ZnO), and 3.82 eV (ITO). These results are consistent with the reports.²¹ Generally, a lower band gap means a higher crystalline degree for ZnO,^{22,23} so the ZnO film processed from the aqueous solution method has a better crystalline quality than processed from the sol-gel method, which is a reason of the good performance of the device with ZnO films processed from the aqueous solution method.

Figure 7 shows the PL spectra of the ZnO films annealed at different temperatures. The intrinsic peak at the 350–400 nm range is related to the near band edge emission of ZnO. The sol-gel processed ZnO layer annealed at 350 °C shows the highest intrinsic peak, the aqueous solution processed ZnO layer annealed at 150 °C shows a reduced intrinsic peak, and the sol-gel processed ZnO layer annealed at 150 °C shows the lowest intrinsic peak. A higher intrinsic peak means a better crystalline quality. Therefore, the crystalline quality sequence is the ZnO layer annealed at 350 °C (the sol-gel method) > 150 °C (the aqueous solution method) > 150 °C (the sol-gel method). The results are consistent with the transmittance spectra. Besides, the wide peaks at the 500–800 nm range are due to the defects, including Zn_i (interstitial Zn atom), O_i , V_O (oxygen atom vacancy), V_{Zn} , V_O^+ , V_O^{+2} , and so on.^{24–26} By comparing the defect related peaks and the intrinsic peak, it can be found that the sol gel processed ZnO film annealed at 350 °C has the fewest amount of defects, the aqueous processed ZnO film annealed at 150 °C has increased defects and the sol-gel processed ZnO film annealed at 150 °C has the most defects. Thus, 350 °C sol-gel processed ZnO owns the best crystalline quality and the lowest amount of defects. However, due to its higher surface roughness of 45.5 Å, the device with

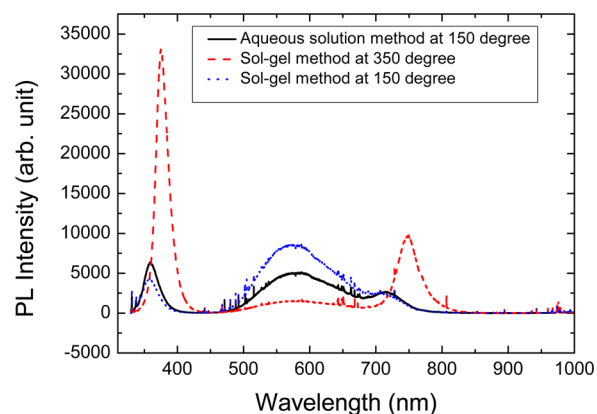


Figure 7. PL spectrum of ZnO thin films that were derived from the sol-gel solution, followed by sintering at 150 °C (red dash line) or 350 °C (blue dot line), or from the aqueous solution, followed by sintering at 150 °C (dark solid line). Devices containing a ZnO layer derived from the sol-gel solution, followed by sintering at 350 °C, own the highest crystalline degree and the relatively lowest amount of defects.

sol-gel processed ZnO annealed at 350 °C only shows a moderate PCE. There is a trade-off between the crystalline quality and the surface roughness. This explains why the device with the aqueous processed ZnO layer shows the best performance.

Recent literatures^{27,28} further demonstrated that two kinds of defects in the ZnO, which are residues of precursors and oxygen related defects, would greatly influence the electrical characteristics of ZnO and lead to the light soaking effect in devices containing ZnO. When the device is soaked in light, ZnO will photocatalyze the decomposition of residual organics that are left by the incomplete conversion of precursors, for instance $Zn(Ac)_2$ in the adopted sol-gel method. As a result, the morphology and conductivity of ZnO^{29,30} will be improved, so the PCE becomes better at the same time. Since the annealing temperature in the adopted sol-gel method is very low and time is only half an hour, further elevating the annealing temperature and extending the annealing time are assumed to make the conversion more complete. The prepared ZnO film generally has oxygen related defects, which will act as traps for electrons and is ascribed as an important reason for the light soaking effect. When the device is soaked in light, oxygen will be desorbed from the ZnO and redistribute in the layer, which causes the light-soaking effect.^{27,28} From the PL and transmittance spectra, it is demonstrated that the sol-gel processed ZnO film annealed at 150 °C has the highest amount of defects, including oxygen related defects. These may be another reason why the device containing a sol gel low temperature ZnO film meets serious light soaking effect. To solve the light-soaking effect caused by the second kind of defects in the sol-gel method, pretreatments, including doping Al into the precursor solution,^{31,32} is generally useful. However, a relatively high annealing temperature,^{13,31} compared with the adopted aqueous solution method, is still a problem. Therefore the adopted aqueous solution method is a more promising method to help us synthesize higher quality ZnO films and get rid of the light soaking effect at a low temperature.

The reliability of the inverted organic solar cell with the aqueous processed ZnO layer was investigated. The devices were stored and measured in air ambient conditions. Figure 8 shows the result of the device with an aqueous processed ZnO

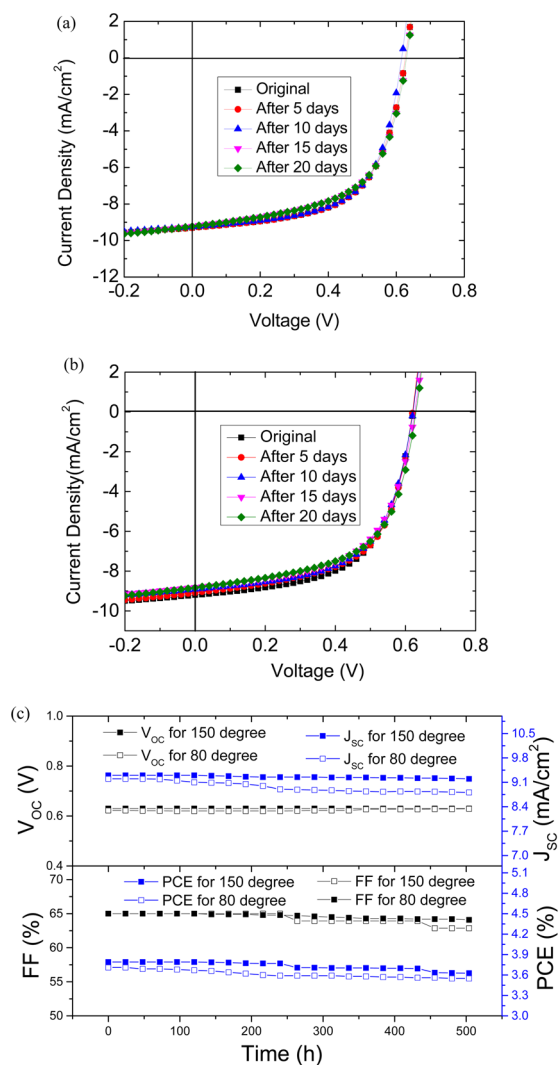


Figure 8. (a) J - V characteristics of the device after stored in air for a different time. The ZnO layer was derived from the aqueous solution, followed by annealed at 150 °C. (b) J - V characteristics of the device after stored in air for a different time. The ZnO layer was derived from the aqueous solution, followed by annealed at 80 °C. (c) Parameter variations of the device with the time stored in air. The tests were under an AM 1.5G illumination intensity of 100 mW/cm². The PCE can keep higher than 96% after 22 days for both annealing temperatures. V_{OC} keeps stable during the period, while FF and J_{SC} decrease slightly.

layer annealed at 150 or 80 °C. For both annealing temperatures, as the time goes, V_{OC} almost keeps unchanged and only J_{SC} and FF slightly decrease. For the annealing temperature of 150 °C, J_{SC} only drops from 9.3 mA/cm² to 9.2 mA/cm², FF drops from 65% to 63%, and PCE of the device stays above 96% of the original efficiency after 22 days. For the annealing temperature of 80 °C, J_{SC} only drops from 9.2 mA/cm² to 8.8 mA/cm², FF drops from 65% to 64%, and PCE of the device stays above 96% of the original efficiency after 22 days. Therefore, when the aqueous processed ZnO layer is annealed at a temperature above 80 °C, the device shows promising reliability.

CONCLUSION

In summary, the low temperature process is always preferred in the organic solar cell fabrication. To obtain a low temperature

process, the sol-gel and aqueous processed ZnO layers annealed at low temperature were used in the inverted organic solar cells. It is found that when the sol-gel processed ZnO film was annealed at a low temperature of 150 °C, the inverted organic solar cell shows a PCE of only 1.3%, and at the same time an obvious “light-soaking” effect appears. However, for the aqueous processed ZnO layer annealed at 150 °C, the inverted device shows a PCE of 3.79% and even when the ZnO layer is annealed at 80 °C, the device still shows a PCE as high as 3.71%. Moreover, the flexible device with a ZnO layer annealed at 80 °C on PET shows a comparable PCE of 3.56% and only slightly decreases to 3.43% after bent for 1000 times. Simultaneously, no “light-soaking” effect is observed in these devices with the aqueous processed ZnO layers. And more important, these devices show very good performances, including stabilities. AFM measurement shows that the aqueous-processed low temperature ZnO layer has a small surface roughness, and meanwhile transmittance spectra and PL spectra measurements also show that it has a good optical properties and film quality, which guarantee the corresponding superior device performance as the electrical characterization has shown. The aqueous solution method is a more promising low temperature technique, compared with the sol-gel method.

AUTHOR INFORMATION

Corresponding Authors

*Fax: 86-29-88201660. Tel: 86-29-88201660. E-mail: cfzhang@xidian.edu.cn.

*Fax: 86-29-88201660. Tel: 86-29-88201660. E-mail: yhao@xidian.edu.cn.

Notes

The authors declare no competing financial interest.

ACKNOWLEDGMENTS

The work is supported by NSFC (611q06063) and the Fundamental Research Funds for the Central Universities (K50511250003).

REFERENCES

- (1) Park, H.-Y.; Lim, D.; Kim, K.-D.; Jang, S.-Y. *J. Mater. Chem. A* **2013**, *1* (21), 6327–6334.
- (2) You, J.; Chen, C. C.; Hong, Z.; Yoshimura, K.; Ohya, K.; Xu, R.; Ye, S.; Gao, J.; Li, G.; Yang, Y. *Adv. Mater.* **2013**, *25* (29), 3973–3978.
- (3) Dang, X.-D.; Dante, M.; Nguyen, T.-Q. *Appl. Phys. Lett.* **2008**, *93* (24), 241911–241911–3.
- (4) Norrman, K.; Gevorgyan, S. A.; Krebs, F. C. *ACS Appl. Mater. Interfaces* **2008**, *1* (1), 102–112.
- (5) Wong, K.; Yip, H.; Luo, Y.; Wong, K.; Lau, W.; Low, K.; Chow, H.; Gao, Z.; Yeung, W.; Chang, C. *Appl. Phys. Lett.* **2002**, *80* (15), 2788–2790.
- (6) Hau, S. K.; Yip, H.-L.; Baek, N. S.; Zou, J.; O'Malley, K.; Jen, A. K.-Y. *Appl. Phys. Lett.* **2008**, *92*, 253301.
- (7) Chen, D.; Zhang, C.; Wang, Z.; Zhang, J.; Feng, Q.; Xu, S.; Zhou, X.; Hao, Y. *IEEE Trans. Electron Devices* **2013**, *60*, 451–457.
- (8) Hoye, R. L.; Muñoz-Rojas, D.; Iza, D. C.; Musselman, K. P.; MacManus-Driscoll, J. L. *Sol. Energ. Mater. Sol. C* **2013**, *116*, 197–202.
- (9) Kim, J.-R.; Cho, J. M.; Lee, A.; Chae, E. A.; Park, J.-U.; Byun, W.-B.; Lee, S. K.; Lee, J.-C.; So, W.-W.; Yoo, S. *Curr. Appl. Phys.* **2011**, *11* (1), S175–S178.
- (10) Park, Y.; Noh, S.; Lee, D.; Kim, J.; Lee, C. *Mol. Cryst. Liq. Cryst.* **2011**, *538* (1), 20–27.
- (11) Chang, J.-J.; Lin, Z.; Zhu, C.-X.; Chi, C.; Zhang, J.; Wu, J. *ACS Appl. Mater. Interfaces* **2013**, *5* (14), 6687–6693.

- (12) Kyaw, A. K. K.; Sun, X.; Tan, S. T.; Divayana, Y.; Demir, H. *IEEE J. Sel. Top. Quantum Electron.* **2010**, *16* (6), 1700–1706.
- (13) Oh, H.; Krantz, J.; Litzov, I.; Stubhan, T.; Pinna, L.; Brabec, C. J. *Sol. Energy Mater. Sol. C* **2011**, *95* (8), 2194–2199.
- (14) Krebs, F. C.; Thomann, Y.; Thomann, R.; Andreasen, J. W. *Nanotechnology* **2008**, *19* (42), 424013.
- (15) Meyers, S. T.; Anderson, J. T.; Hung, C. M.; Thompson, J.; Wager, J. F.; Keszler, D. A. *J. Am. Chem. Soc.* **2008**, *130* (51), 17603–17609.
- (16) Bai, S.; Wu, Z.; Xu, X.; Jin, Y.; Sun, B.; Guo, X.; He, S.; Wang, X.; Ye, Z.; Wei, H. *Appl. Phys. Lett.* **2012**, *100* (20), 203906–203906–4.
- (17) Zhang, C.; You, H.; Lin, Z.; Hao, Y. *Jpn. J. Appl. Phys.* **2011**, *50* (8), 082302–1.
- (18) Kim, J.; Kim, G.; Choi, Y.; Lee, J.; Heum Park, S.; Lee, K. J. *Appl. Phys.* **2012**, *111* (11), 114511–114511–9.
- (19) Trost, S.; Zilberberg, K.; Behrendt, A.; Polywka, A.; Görrn, P.; Reckers, P.; Maibach, J.; Mayer, T.; Riedl, T. *Adv. Energy Mater.* **2013**, *3*, 1437–1444.
- (20) Ma, Z.; Tang, Z.; Wang, E.; Andersson, M. R.; Inganas, O.; Zhang, F. *J. Phys. Chem. C* **2012**, *116* (46), 24462–24468.
- (21) Shan, F.; Yu, Y. *J. Eur. Ceram. Soc.* **2004**, *24* (6), 1869–1872.
- (22) Tan, S.; Chen, B.; Sun, X.; Fan, W.; Kwok, H.; Zhang, X.; Chua, S. *J. Appl. Phys.* **2005**, *98* (1), 013505–013505–5.
- (23) Tan, S.; Chen, B.; Sun, X.; Hu, X.; Zhang, X.; Chua, S. *J. Cryst. Growth* **2005**, *281* (2), 571–576.
- (24) Panigrahy, B.; Aslam, M.; Misra, D. S.; Ghosh, M.; Bahadur, D. *Adv. Funct. Mater.* **2010**, *20* (7), 1161–1165.
- (25) Kushwaha, A.; Aslam, M. *J. Appl. Phys.* **2012**, *112* (5), 054316–054316–7.
- (26) Wu, X.; Siu, G.; Fu, C.; Ong, H. *Appl. Phys. Lett.* **2001**, *78* (16), 2285–2287.
- (27) Lilliedal, M. R.; Medford, A. J.; Madsen, M. V.; Norrman, K.; Krebs, F. C. *Sol. Energy Mater. Sol. C* **2010**, *94* (12), 2018–2031.
- (28) Krebs, F. C.; Tromholt, T.; Jorgensen, M. *Nanoscale* **2010**, *2* (6), 873–886.
- (29) Yang, J.; Chen, C.; Ji, H.; Ma, W.; Zhao, J. *J. Phys. Chem. B* **2005**, *109* (46), 21900–21907.
- (30) Wu, T.; Lin, T.; Zhao, J.; Hidaka, H.; Serpone, N. *Environ. Sci. Technol.* **1999**, *33* (9), 1379–1387.
- (31) Sondergaard, R.; Helgesen, M.; Jorgensen, M.; Krebs, F. C. *Adv. Energy Mater.* **2011**, *1* (1), 68–71.
- (32) Alstrup, J.; Jorgensen, M.; Medford, A. J.; Krebs, F. C. *ACS Appl. Mater. Interfaces* **2010**, *2* (10), 2819–2827.